Materials Research. 2017; 20(4): 973-983
DOI: http://dx.doi.org/10.1590/1980-5373-MR-2016-0467

Preparation, Characterization and Biological Studies of B-TCP and B-TCP/Al_2O_3 Scaffolds Obtained by Gel-Casting of Foams

Lilian Siqueira[a], Cynthia Guimarães de Paula[a], Mariana Motisuke[a], Rubia Figueredo Gouveia[b], Samira Esteves Afonso Camargo[c], Noala Vicensoto Moreira Milhan[c], Eliandra de Sousa Trichês[a]*

[a] Bioceramics Laboratory (BIOCERAM), Science and Technology Institute - ICT, Universidade Federal de São Paulo – UNIFESP, 330 Talim St, Zip Code 12231-280, São José dos Campos, SP, Brazil
[b] Brazilian Nanotechnology National Laboratory (LNNANO), Centro Nacional de Pesquisa em Energia e Materiais - CNPEM, P.O. Box 6192, 13083-970, Campinas, SP, Brazil.
[c] Department of Biosciences and Oral Diagnosis, School of Dentistry, Universidade Estadual Paulista "Júlio de Mesquita Filho" - UNESP, 777 Engenheiro Francisco José Longo Avenue, Zip Code 12245-000, São José dos Campos, SP, Brazil

Received: June 19, 2016; Revised: October 04, 2016; Accepted: April 25, 2017

Replacement tissues for tissue engineering can be produced by seeding human cells onto scaffolds. In order to guarantee adequate bio-compatibility, porosity and mechanical resistance for promoting cellular growth, proliferation and differentiation within scaffold structures, it is necessary to investigate and improve materials and processing routes. β-tricalcium phosphate can be considered a very suitable bio-ceramic material for bone therapy because of its biocompatibility, osteo-conductivity and neo-vascularization potential. Alumina is commonly used as a sintering additive. In this study, β-TCP and β-TCP/Al_2O_3 scaffolds were obtained by gel-casting method. The scaffolds showed high porosity (86-88%) and pore sizes ranging from 200 to 500 μm. Even though alumina did not promote improvement in β-TCP/Al_2O_3 scaffolds in terms of mechanical performance, they showed great cytocompatibility as there was no cytotoxic and genotoxic effect. Therefore, β-TCP and β-TCP/Al_2O_3 scaffolds are good candidates for application in tissue engineering.

Keywords: *Tricalcium phosphate; alumina; gel-casting method; cytocompatibility; scaffolds*

1. Introduction

Tissue engineering is a scientific field that integrates biological components, such as cells and growth factors, with engineering principles and synthetic materials. Therefore, as an interdisciplinary field, tissue engineering concerns the development of biological substitutes capable of replacing or repairing diseased or damaged tissue and organs in humans[1-4]. Since the 80's, and especially in the last decade, tissue engineering and regenerative medicine have been proving its importance and potential to revolutionize important areas of medicine[1-4], such as cardiovascular[5-6], skin regeneration[7] and bone treatments[8-11].

Replacement tissues can be produced by first seeding human cells onto scaffolds[1-4]. Scaffolds are temporary support structures that provide adequate conditions for cell proliferation, migration, and differentiation in 3D, allowing formation of specific tissues with appropriate functions. Some common properties of an ideal scaffold for tissue engineering are biocompatibility, porosity with interconnected pores and adequate mechanical strength, depending mainly on the tissue to be repaired [1-2,4,10-11].

An ideal scaffold porosity is required to maximize the space for cellular adhesion, growth, revascularization, adequate nutrition and other factors that can influence cellular and tissue growth[1-4,9-10]. Different methods have been studied and improved in the past years to obtain scaffolds with desired properties[1,10], such as porogen particles[12], emulsion[13-15], replication[8,16], gel-casting of foams[12,14,16-18] and additive manufacture[19].

Gel-casting method consists in adding a foaming agent to a ceramic suspension composed of ceramic powder, organic monomers and dispersants, thus providing a mechanical action. After gelation of the foam due to *in situ* polymerization of water-soluble monomers (previously added to the ceramic suspension) and its sintering, some of the scaffold properties produced were: ideal porosity (40–90%) and porous morphology with spherical-shaped pores measuring between 50 and 800 mm, and thick walls with homogeneous micro-structure, thus improving the mechanical properties of these materials, which can help cellular growth. Furthermore, this method is cheaper than others and does not require atmospheric control[20-23].

* e-mail: eliandra.sousa@unifesp.br

Bone scaffolds can have an optimal performance so long as they can be bio-degradable, bio-resorbable and capable of providing mechanical support for repair and regeneration of diseased or damaged bone while the growing tissue replaces the scaffold[1-4,9-10].

There are many ceramic materials that have been used for bone tissue engineering, such as calcium phosphates, especially hydroxyapatite (HA)[1,12,16,18] and β-tricalcium phosphate (β-TCP)[1,8,16], bioactive glass[24,25] and titania[26]. Tricalcium phosphate (TCP) is a bio-resorbable, bio-active and osteo-conductive bio-ceramic material. Also, the β-TCP phase, one of its four polymorphic phases, stands out due to its solubility, degradation rate and higher angiogenic activity compared to other calcium phosphates, which is highly related to the process of neo-vascularization of new tissues[27-32].

Unfortunately, β-TCP undergoes a β→α polymorphic transformation while being processed, which takes place at temperatures as low as 1150 ºC[28,32]. As a straightforward consequence, a poor mechanical performance (e.g. compressive strength) attributed to porous structures is more pronounced, limiting its application. Also, the porosity increases the complexity for manufacturing reproducible scaffolds.

One way to improve such mechanical properties would be to use sintering additives, which could improve the thermal stability of β-TCP or form a liquid phase during sintering, either process favoring material densification[33-36]. Among the various additives (e.g. alumina, titania, calcium pyrophosphate, zirconium, magnesium and others), alumina stands out due to the combination of its excellent corrosion resistance, good bio-compatibility, high wear resistance, high compressive strength and high hardness[37]. For this reason, alumina is commonly used to improve β-TCP densification during sintering[35].

In the literature, there are few reports about bio-ceramic materials produced by gel-casting method[17,38-39]. Thus, this manuscript makes a scientific contribution to the processing of bio-ceramic materials with high porosity, adequate sphericity and high interconnectivity all desirable characteristics for a good scaffold.

Based on this context, the current work reports the preparation of β-TCP and β-TCP/Al_2O_3 scaffolds by using gel-casting of foams with appropriate porosity, interconnectivity and bio-active behavior for application in tissue engineering.

2. Materials and Methods

2.1. Fabrication of β-TCP and β-TCP/Al_2O_3 scaffolds

β-TCP powder was synthesized by means of solid-state reaction at 1050 ºC from an appropriate mixture of calcium carbonate ($CaCO_3$ – Synth) and calcium phosphate ($CaHPO_4$ – Synth), as already published elsewhere[40]. The resulting powder was ballmilled for 48 hours (alumina grinding media with 10 mm spheres at ball/powder ratio of 10:1) and presented a mean size of 3.4 μm and particle size distribution of 0.3-26 μm.

β-TCP and β-TCP/Al_2O_3 scaffolds were fabricated by using the gel-casting method. Ceramic slurries with solid content of 35 vol.-% were prepared by dispersing β-TCP powder in an aqueous solution containing 15 vol.-% of organic monomers (methacrylamide - MAM, Sigma-Aldrich, N,N,N',N'-hydroxymethyl acrylamide - HMAM, Sigma-Aldrich and methylenebisacrylamide - MBAM, Sigma-Aldrich) at a molar ratio of 3:3:1 (MAM:HAMAM:MBAM). Ammonium polymethacrylate (Darvan® C-N, R.T. Vanderbilt Company, Inc.) was used as dispersant agent. Different amounts of alumina (5, 10 and 15 wt.-%) (Al_2O_3 – Alcoa, A 1000-SG, Alcoa, d_{50} = 0.5 μm, ρ = 2.98 $g.cm^{-3}$) were added to produce the β-TCP/Al_2O_3 scaffolds. The slurries were finally homogenized with ball mills for 15 minutes.

To produce the foam, non-ionic surfactant (Lutensol ON-110, BASF) was added to the slurry before being stirred for 2 minutes with a mixer. Ammonium persulfate (APS, Vetec) and N,N,N,N′-tetramethylethylenediamine (TEMED, Sigma-Aldrich) were used as initiator and catalyst for gelation reaction, respectively. The foams were dried at 50 ºC for 24 hours and then the samples were core-drilled (cylinders, d = 7 mm and h = 14 mm). Heat treatment was performed as follows: samples were fired at 500 ºC (heating rate of 1 ºC/min and dwell time of 1 hour) to eliminate all organic components; next, sintering was made at temperature of 1200 ºC (heating rate of 5 ºC/min and dwell time of 2 hours).

2.2. Characterization

β-TCP and β-TCP/Al_2O_3 scaffolds were analyzed by X-ray diffraction (Shimadzu XRD7000, CuKα radiation, 2θ = 20-40º, 30 mA, 40 k). The JCPDS database files used to identify the crystalline phases formed were 09-0169 for β-TCP, 09-0348 for α-TCP and 10-0173 for Al_2O_3. The fracture surface of the sintered scaffolds was observed by using a scanning electron microscope (JEOL JSM6360-LV). The total porosity of the scaffolds was determined according to Equation (1)[41]. The geometric density ($\rho_{scaffold}$) of the cylindrical samples was calculated by using their dimensions (height and diameter) and weight. The theoretical density (ρ_{He}) was calculated for each formulation according to Equation (2), where $\rho_{\beta\text{-}TCP}$ and ρ_{Al2O3} are the theoretical densities of β-TCP (3.07 g/cm^3) and Al_2O_3 (3.98 g/cm^3), respectively. X β-TCP and X Al_2O_3 are the mass fractions of each phase added.

$$P(\%) = 1 - \left(\frac{\rho_{scaffold}}{\rho_{He}}\right) \times 100 \qquad (1)$$

$$\rho_{He} = \rho_{\beta-TCP} \times X_{\beta-TCP} + \rho_{Al_2O_3} \times X_{Al_2O_3} \qquad (2)$$

X-ray microtomographic images of β-TCP and β-TCP/Al_2O_3 scaffolds were obtained by using a high resolution

X-ray microtomograph (SkyScan 1272 Bruker microCT, Kontich, Belgium) operating at 30 kV and 160 µA. The nominal resolution of 6.5 µm was obtained by using X-ray detector of 1224 x 820 pixels. NRecon software (Software Version 1.6.9.8, Bruker MicroCT®) was used to reconstruct cross-section images from microtomographic projections into 3D images based on the Feldkamp algorithm. The same electronic density contrast was selected for all samples in order to allow comparisons. The 3D images were viewed with CTVOX software (Version 2.7.0, Bruker MicroCT®), whereas 2D images *per* slices were obtained with Dataviewer software (Version 1.5.1.2, Bruker MicroCT®). Total porosity and pore size distribution were quantified by using the CT analyzer software (Version 1.14.4.1, Bruker MicroCT®). For acquisition of porosity parameters, the volume object of interest (VOI) was previously set to 4 mm^3.

The compressive strength of at least ten cylindrical samples (h/d = 2) was determined by using a universal testing machine (EMIC DL2000) at cross-head speed of 0.5 $mm.min^{-1}$.

2.3. Biological tests

In this study, osteoblast-like cells (MG 63) were obtained from the Rio de Janeiro Cell Bank (Rio de Janeiro, RJ, Brazil). The cells were cultured in DMEM (Cultilab Curitiba, Brazil), supplemented with 10% fetal bovine serum (FBS), penicillin (100 UI/mL), streptomycin (100 µg/mL) and then maintained at 37 °C and 5% of CO_2. Cell culture flasks of 75 mL and 250 cm^2 were used. The culture medium was changed every two days and the cell growth was assessed by using a reverse phase microscope (Microlimaging GmbH - Axiovert 40C, Carl Zeiss Microscope, Jena, Germany).

2.3.1 Cell attachment

For assessment of cell attachment and morphology of the cells in contact with the scaffolds, these were placed in 24-well plates and the cells plated on them before being maintained at 37 *°C and 5% CO_2*. After 3-day growth of MG63 on the scaffolds, the cells were investigated by using SEM (Inspect S50, FEI Company, Brno, Czech Republic). For this, the culture medium was removed and the scaffolds were twice rinsed with PBS. The cells adhered in the scaffolds were fixed with 0.25% glutaraldehyde and 4% paraformaldehyde diluted in PBS before being dehydrated by a series of ascending ethanol concentrations (70%, 80%, 90% and 100% for 10 minutes each). Next, the scaffolds were air-dried at room temperature for 24 hours. For SEM examination, the scaffolds were sputter-coated with palladium-gold alloy (Polaron SC 7620 Sputter Coater, Quorum Technologies, Newhaven, UK) at a thickness of 7-10 nm (10-15 mA, under a vacuum of 130 mTorr), with scanning electron microscope operating between 15-30 kV and spot 7.

2.3.2 Cytotoxicity

For the cytotoxicity test, $2x10^4$ cells were plated in 24-well plates and maintained at 37 °C and 5% CO_2. After 24 hours, the scaffolds were placed on the cells and the plates maintained at 37 °C and 5% CO_2 for further 24 hours. Next, the viability of the cells put in contact with the scaffolds was determined by MTT assay (3-(4,5 dimethylthiazol-2-yl)-2,5-diphenyltetrazolium bromide, Sigma, St Louis, MO, USA), which is a test that evaluates not only the number of cells, but also the level of their metabolic activity as it is based on the activity of enzymes, such as succicil dehydrogenase, present in viable cells[42]. MTT solution was added to each well and the cells were incubated for 1 hour. Next, DMSO (dimethyl sulfoxide solvent, Sigma-Aldrich, St Louis, MO, USA) was also added to each well and the plates were shaken at room temperature for 10 minutes. The resulting optical density was measured in a spectrophotometer (Biotek-EL808IU, BioTek Instruments, Inc., Winooski, VT, USA) at 570 nm. The cytotoxicity was expressed as a percentage of the control group (100%) and the differences between values were statistically analyzed by ANOVA ($P \leq 0.05$).

2.3.3 Genotoxicity

For assessment of the genotoxicity, $2x10^4$ cells were plated in 24-well plates and maintained at 37 *°C and 5% CO_2* for 24 hours. After this period, the scaffolds were placed on the cells and the plates were maintained at 37 *°C and 5% CO_2* for further 24 hours. Next, the scaffolds were removed from the plates and the cells were rinsed with PBS and fixed with 4% paraformaldehyde diluted in PBS for 10 minutes. PBS and Fluroshield with DAPI solution (Sigma, St Louis, MO, USA) were added to each well and the nuclei of the cells were observed by means of immunofluorescence and then photographed with a digital camera (Sony F828 Digital, CyberShot, 8.0 megapixels) coupled to an inverted light microscope (Carl Zeiss Microscope Micro lmaging GmbH - Axiovert 40C, Germany). The micronucleus test is based on the loss of chromosomes or their fragments during cell mitosis. Entire chromosomes or their fragments not reincorporated by the nucleus after cell division lead to micronuclei formation[43]. A cell counter (Image J software) was used to assist in the counting of micronuclei. The micronuclei were determined microscopically at 1,000 cells/well and the differences between the values were statistically analyzed by using Mann-Whitney U test ($P \leq 0.05$).

3. Results and Discussion

Figure 1 shows XRD patterns of the β-TCP and β-TCP/Al_2O_3 scaffolds. Only β-TCP crystalline phase (JCPDS 09-0169) was observed for β-TCP scaffold, whereas alumina

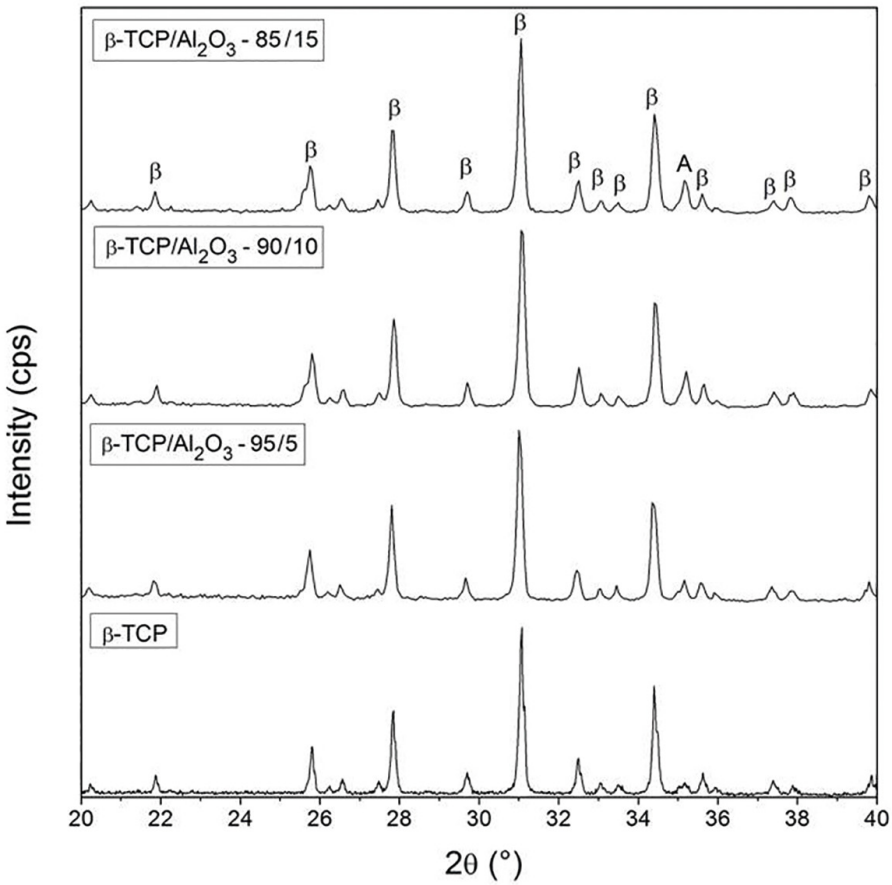

Figure 1. XDR patterns of the β-TCP and β-TCP/Al_2O_3 scaffolds. β=β-TCP; A=Al_2O_3.

(JCPDS 10-0173) was identified in all β-TCP/Al_2O_3 scaffolds (2θ = 35.13º, 43.36º and 57.51º).

Figure 2 presents SEM micrographs of the fracture surface of the β-TCP and β-TCP/Al_2O_3 scaffolds. All scaffolds (Figure 2-B1, C1 and D1) presented homogeneous macro-structure with spherical and interconnected pores. The mean pore size varied from 200 to 500 μm, which is considered adequate for bone tissue growth[11,27]. For β-TCP scaffolds, it is possible to observe an inter-granular porosity. With regard to β-TCP/Al_2O_3 scaffolds, alumina particles filled the micro-porosity of the scaffolds, as can be seen in Figure 2 (B2-B3, C2-C3 and D2-D3). It can also be observed that the micro-structure of the scaffolds consists of two phases: calcium phosphate and small grains related to alumina. These results are in agreement with those reported by Ayed and Bouaziz[35], who studied the effect of alumina addition on densification of tricalcium phosphate-26.52 wt.-% fluorapatite composites.

Furthermore, in another study, high-density tricalcium phosphate-26.52 wt.-% fluorapatite-20 wt.-% zirconia composites were produced after sintering at various temperatures[44]. The authors observed that high temperatures (above 1300 ºC) or mass percentages of zirconia (near 20 wt.-%) are not the best conditions for composite densification. This is probably due to the new compound formation (CZ and TTCP). Also, it was observed that partial decomposition of TCP increases during the sintering process by the addition of zirconia (near 20 wt.-%) at 1400 °C.

Table 1 shows the porosity values for β-TCP and β-TCP/Al_2O_3 scaffolds, whose geometric porosities varied from 86 to 88%, values higher than those reported in the literature. Therefore, the processing route influences the properties of the scaffolds. The comparison carried out here is between scaffolds made of other bioactive ceramic and high-porosity glass materials (~70%) and prepared by gel-casting method. Therefore, few reports were found. For example, Rehman and Zhang prepared hydroxyapatite scaffolds with porosities ranging from 70 to 77% by combining gel-casting and replica methods [45]. Wu and collaborators produced bio-glass scaffolds with 74-84% porosity by using a modified gel-casting of foams[46].

The porosity of β-TCP and β-TCP/Al_2O_3 scaffolds determined by microtomography varied from 70 to 77%, values lower than those obtained by geometric porosity for

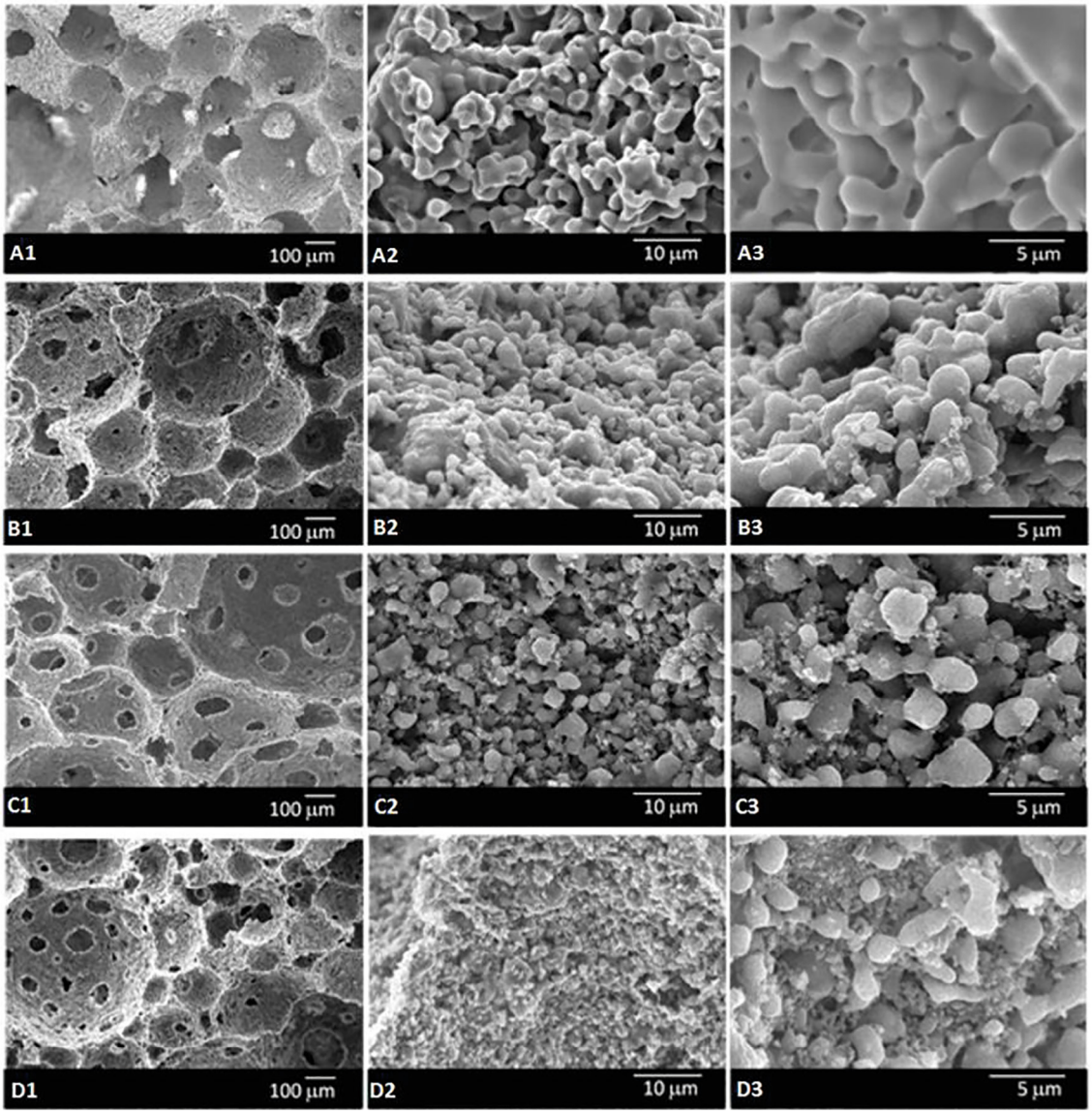

Figure 2. SEM micrographs of β-TCP and β-TCP/Al_2O_3 scaffolds. (A1, A2, A3) β-TCP, (B1, B2, B3) β-TCP/Al_2O_3 – 95/5, (C1, C2, C3) β-TCP/Al_2O_3 – 90/10 and (D1, D2, D3) β-TCP/Al_2O_3 – 85/15.

all scaffolds. This result was already expected as meso- and nano-pores can be calculated by this method.

Moreover, it is necessary to point out that the presence of alumina does not influence the scaffold porosity.

X-ray microtomographic images were also used to obtain 3D images of the scaffolds, as shown in Figure 3. The color bar is proportional to the attenuation of X-rays passing through the scaffolds: colors on the left side show lower attenuation than those on the right side. The attenuation is influenced by changes in the sample, such as thickness, density and electronic density (basically, the atomic number of the involved samples). No significant changes in the micro-structures were observed in the scaffolds.

Different cross-sections of these images (Figure 4) provide a two-dimensional visualization of the interior of the scaffolds, showing a highly porous material.

Figure 5 presents the 3D model obtained (Figure 3) and its pore size distribution. All samples show a wide pore size distribution, as observed in the SEM images, as well as similar porosity, confirming that alumina acts mainly as a filler for β-TCP grains.

Table 2 shows the compressive strength of β-TCP and β-TCP/Al_2O_3 scaffolds. By comparing between β-TCP and β-TCP/Al_2O_3 scaffolds, alumina did not improve the mechanical resistance of the former. This fact can be associated to the great difference in the sintering temperature of both powders. Another

Table 1. Porosity of β-TCP and β-TCP/Al_2O_3 scaffolds.

Methods	Porosity (%) Concentration of alumina (%)			
	0	5	10	15
Geometrical	86.4 ± 1.0	87.1 ± 0.7	87.6 ± 0.7	87.5 ± 0.9
Microtomography	70.8 ± 0.3	73 ± 1.0	77 ± 1.0	75 ± 1.0

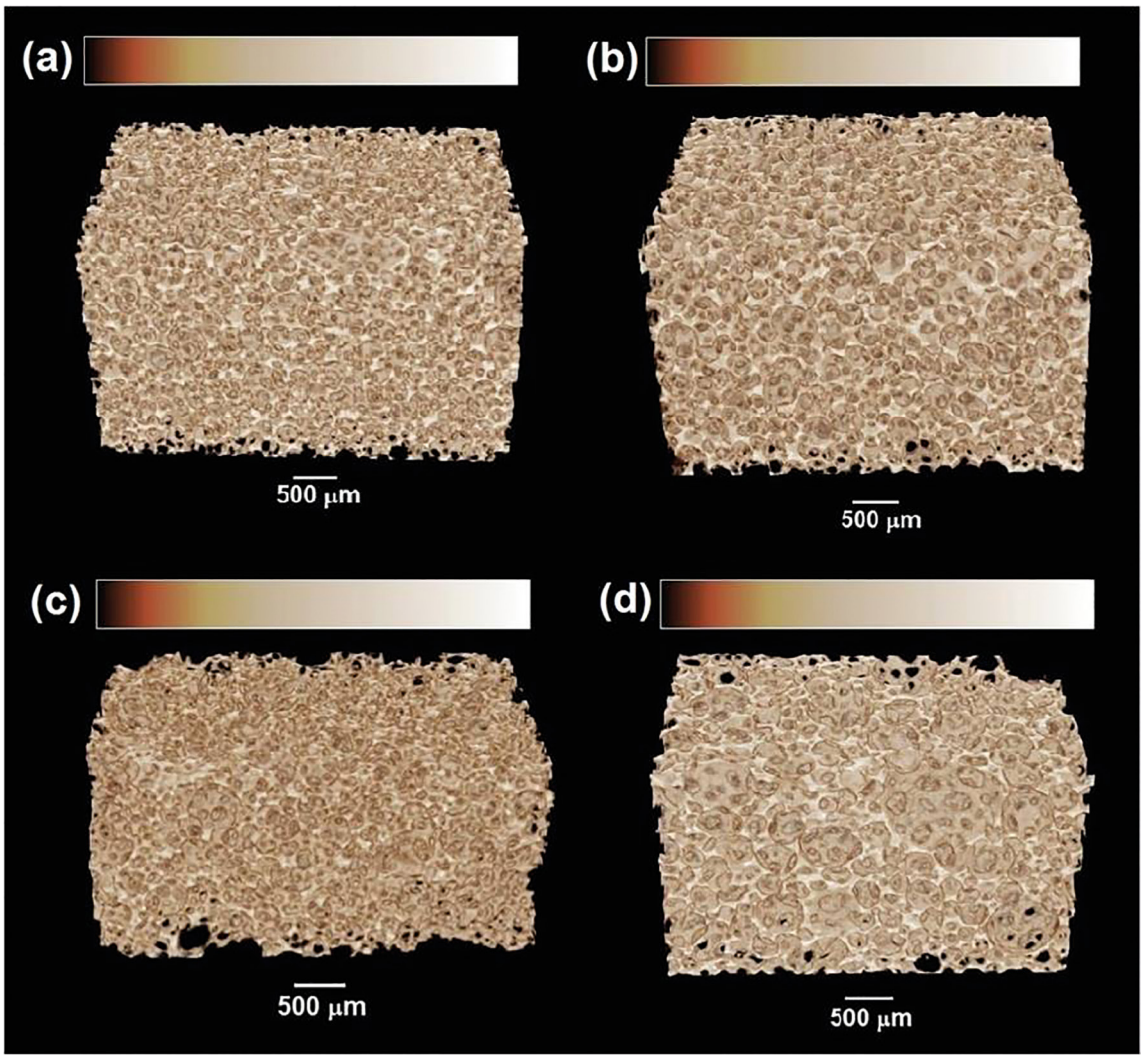

Figure 3. 3D images of the scaffolds obtained by X-ray microtomography: (a) β-TCP; (b) β-TCP/Al_2O_3 – 95/5; (c) β-TCP/Al_2O_3– 90/10 and (d) β-TCP/$A_{l2}O_3$ – 85/15.

possibility could be the size of alumina particles, which are still in micrometer scale. In the literature, it is known that alumina particles are commonly used in micro-nanometric scale to improve the β-TCP densification during the sintering step. In the case of micrometric particles, these should be used in small amounts (≤ 2.5 wt.-%). This was confirmed by Bouslama et al., who used alumina as a promising material for reinforcement of calcium phosphate[47].In their study, the mechanical properties of the β-TCP-fluorapatite composite was improved by adding 2.5 wt.-% micro-sized alumina powder as additive.

In recent years, the use of nano-sized ceramic additives for strengthening bone substitutes has been studied. In the study by Ghzanfari et al.[48], the effect of nano-alumina content on phase transformation and micro-structural and mechanical properties of HA/nAl_2O_3 scaffolds, fabricated by the freeze-casting method, was evaluated. Their results showed that the decomposition of HA to TCP was accelerated by increasing the nAl_2O_3 content at sintering temperature. In addition, the increase in the nAl_2O_3 content increased the pore size and the compressive strength of the scaffolds.

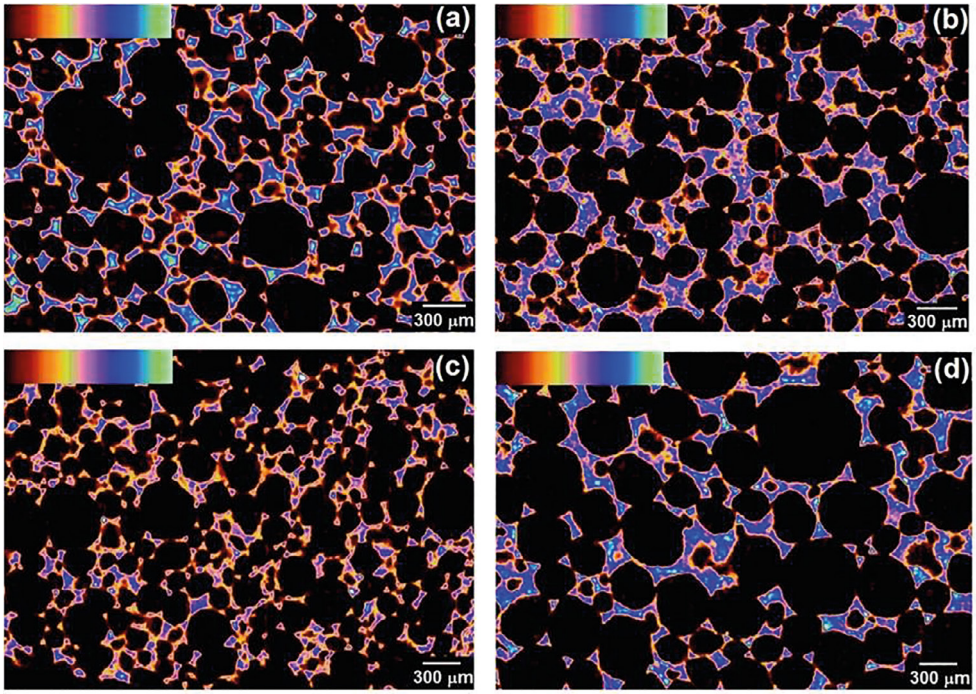

Figure 4. 2D slices of the 3D images obtained by X-ray microtomography: (a) β-TCP; (b) β-TCP/Al_2O_3 – 95/5; (c) β-TCP/Al_2O_3 – 90/10 and (d) β-TCP/Al_2O_3 – 85/15.

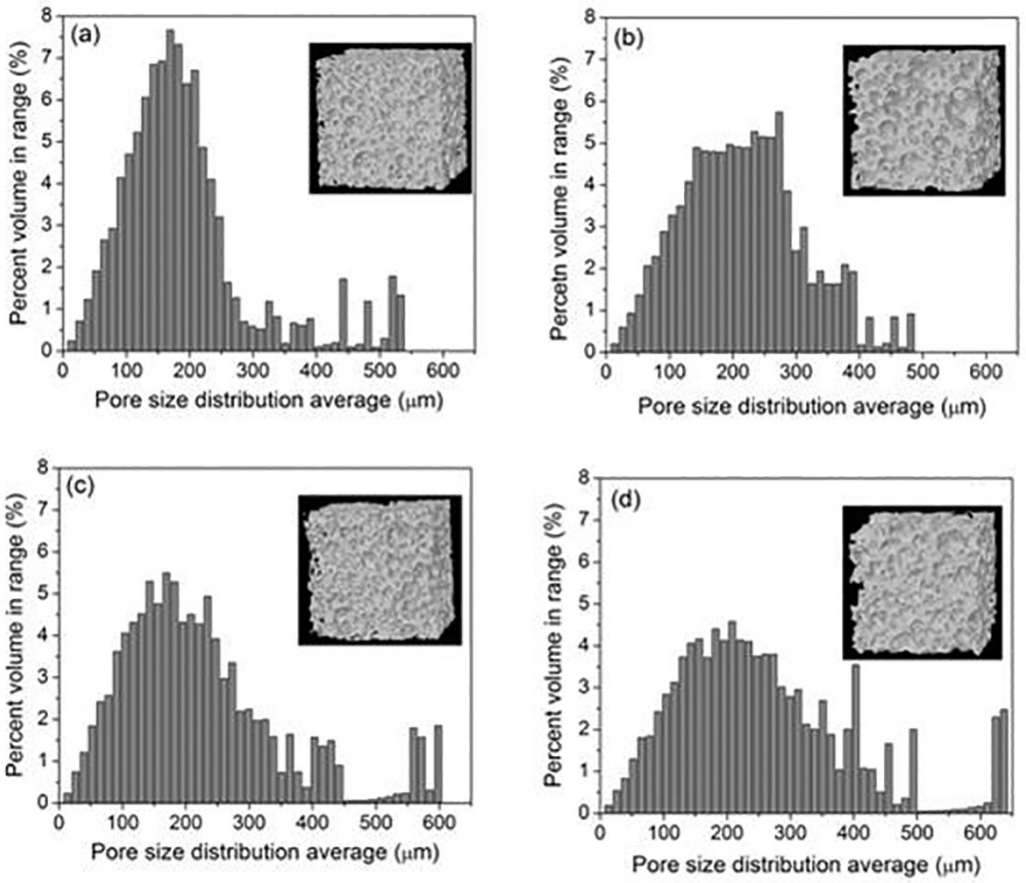

Figure 5. 3D model re-constructed and mean pore size distribution for the scaffolds presented in Figure 3: (a) β-TCP; (b) β-TCP/Al_2O_3– 95/5; (c) β-TCP/Al_2O_3 – 90/10 and (d) β-TCP/Al_2O_3 – 85/15.

Table 2. Compressive strength of β-TCP and β-TCP/Al_2O_3 scaffolds.

	Concentration of alumina (%)			
	0	5	10	15
Compressive strength (MPa)	0.37 ±0.05	0.21 ± 0.05	0.23 ±0.08	0.17 ±0.03

In another study, Hesaraki et al.[49] studied the addition of alumina and silica nano-particles to produce beta-tricalcium phosphate scaffolds, resulting in improved mechanical and biological properties.

Therefore, we intend to use nano-sized particles in further works to obtain bio-ceramic scaffolds by gel-casting method, since this method is still little explored in the literature and allows the production of highly porous scaffolds with highly interconnected spherical pores, which would promote cell growth within the structure.

As it is known, porosity and mechanical strength are inversely proportional properties. Therefore, the low values found for the mechanical strength of β-TCP and β-TCP/Al_2O_3 scaffolds were already expected. However, our results indicated that the compressive strength of ~0.2–0.4 MPa is sufficient for the scaffolds to be handled and manipulated during all tests. The compressive strength of spongy bone is in the range of 0.2–4.0 MPa when the relative density is 0.1[50]. Hence, the compressive strength of the present scaffolds falls in this range, but lies closer to the lower bound. It has also been speculated that it might not be necessary to fabricate a scaffold with mechanical strength equal to that of bone because cells cultured on scaffolds and *in vitro* formation of new tissues will create a bio-composite and will increase the time-dependent strength of the scaffold significantly[25].

Cell attachment was observed in all scaffolds. There was an intimate contact between the cells as they were scattered all over the surface (Figure 6).

Cell viability was analyzed by MTT assay and the average percentages of absorbance values measured for each concentration are shown in Figure 7. The data obtained in this test were statistically analyzed by using ANOVA, which showed that there was no statistical difference between control (100%) and experimental groups ($P > 0.05$). Thus, none of the concentrations tested was found to be cytotoxic to the cells. Moreover, there was no statistical difference

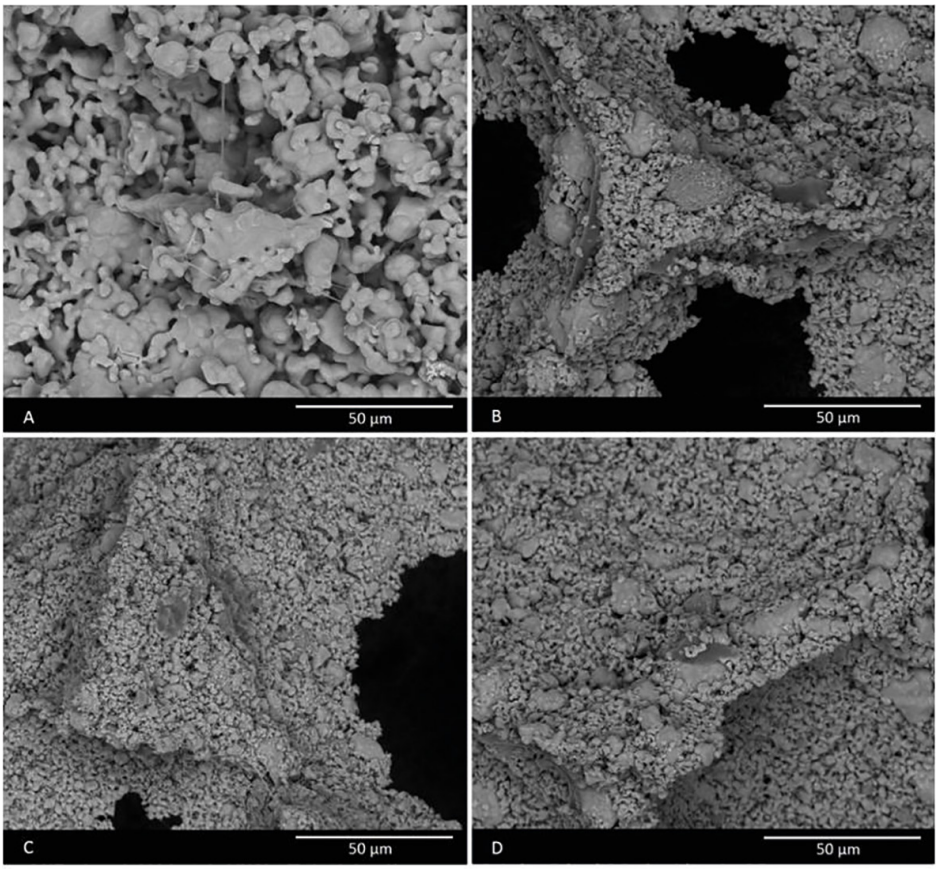

Figure 6. Cell spreading on the samples after 3 days, as observed by SEM: (A) β-TCP; (B) β-TCP/Al_2O_3 – 95/5; (C) β-TCP/Al_2O_3 – 90/10 and (D) β-TCP/Al_2O_3 – 85/15.

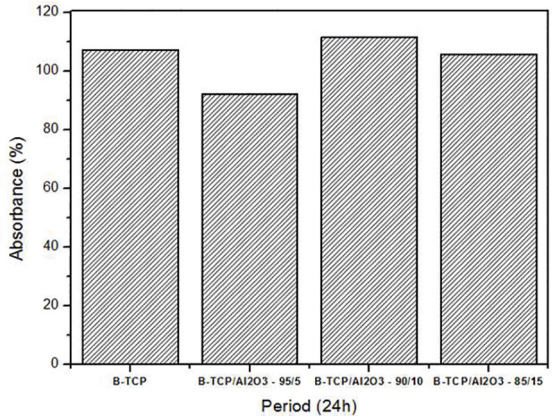

Figure 7. Graph showing mean percentage of absorbance, obtained with MTT assay, after contact of the cells with β-TCP/Al_2O_3 scaffolds for 24 hours.

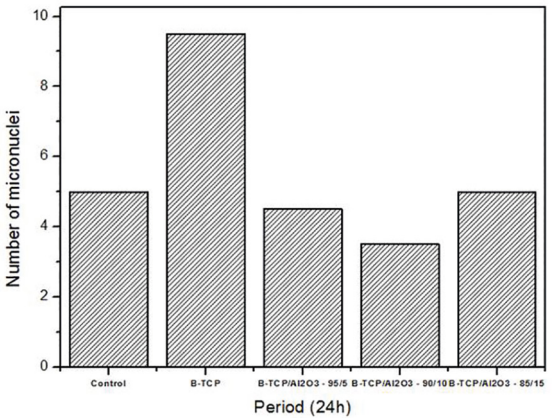

Figure 9. Graph showing number of micronuclei in 1,000 cells/well after contact of the cells with β-TCP/Al_2O_3 scaffolds for 24 hours.

between the groups regarding the amount of alumina used ($P > 0.05$). These results indicate that different amounts of alumina within β-TCP did not affect the cell viability, which was already expected as β-TCP and Al_2O_3 have been investigated and exhibited high biocompatibility[51-53].

Genotoxicity was evaluated in this study through the micronucleus test. The DNA structures contained in the cytoplasm are clearly separated from the main nuclei as their area is 1/3 smaller, thus being considered as micro-nuclei (Figure 8). Only cells containing less than five micronuclei were counted, whereas mitotic and apoptotic cells were not.

The mean number of micronuclei observed in this study (1,000 cells/well) can be observed in Figure 9. There was no statistical difference between control and experimental groups regarding the number of micronuclei ($P > 0.05$), although β-TCP scaffolds have presented the highest number of micronuclei. Furthermore, the groups were not statistically different from each other ($P > 0.05$). These results were already expected as no degree of cytotoxicity had been previously observed in this study and β-TCP scaffold is known to be biocompatible[47]. According to Tsaousi et al.[54], alumina particles are weakly genotoxic only to human cells *in vitro* and the induction of micronuclei is not affected by the size or shape of the particles. However, in our study, different amounts of alumina added to β-TCP scaffold were not found to be genotoxic to the cells.

Based on the results above, β-TCP and β-TCP/Al_2O_3 scaffolds produced by gel-casting method showed good characteristics, such as high porosity, interconnected pores with spherical geometry and pore size in the range of 200-500 μm, which make these scaffolds good candidates for use in tissue engineering.

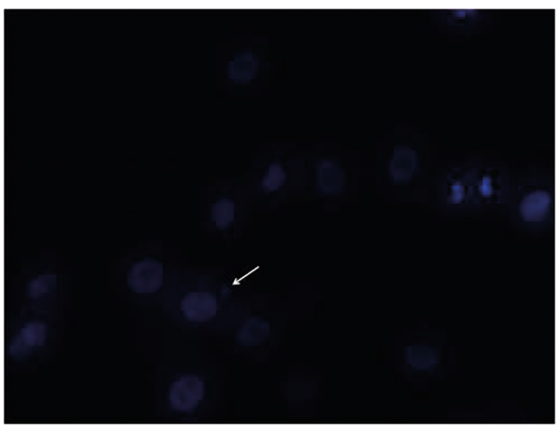

Figure 8. Photomicrography of MG-63 nuclei after contact of the cells with β-TCP/Al_2O_3– 85/15 for 24 hours. Note the presence of a micronucleus (arrow) in this site (Fluroshield with DAPI Immunofluorescence staining; original magnification x20).

4. Conclusions

It was possible to obtain β-TCP and β-TCP/Al_2O_3 scaffolds with high porosity (> 86%) and spherical and interconnected pores by using the gel-casting method. All scaffolds showed cytocompatibility with no cytotoxic and genotoxic effects. These findings indicate a possible application of this β-TCP/Al_2O_3 scaffold for bone tissue engineering.

5. Acknowledgments

The authors would like to thank the São Paulo Research Foundation - FAPESP (Grant: 2010/00863-0) and the National Council for Scientific and Technological Development (Grant: 456461/2014-0 and CNPq/PIBITI/UNIFESP) for the financial support. The authors are also thankful to Prof. Celso A. Bertran from the Institute of Chemistry, University of Campinas (UNICAMP), for supporting XRD and SEM analyses and to the Brazilian Nanotechnology National Laboratory (LNNano) for X-ray microtomography images.

6. References

1. Ikada Y. Challenges in tissue engineering. *J. R. Soc. Interface*. 2006; 3:589–601.

2. Katari RS, Peloso A, Orlando G. Tissue engineering. *Advances in Surgery*. 2014; 48(1):137–154.

3. Fisher MB, Mauck RL. Tissue engineering and regenerative medicine: recent innovations and the transition to translation. *Tissue Eng. Part B Rev*. 2013; 19(1):1–13.

4. Yang S, Leong KK, Du Z, Chua CK. The design of scaffolds for use in tissue engineering. Part I. Traditional Factors. *Tissue Eng*. 2001; 7(6):679–689.

5. Jana S, Tefft BJ, Spoon DB, Simari R.D. Scaffolds for tissue engineering of cardiac valves. *Acta Biomater*. 2014; 10:2877–2893.

6. Fallahiarezoudar E, Ahmadipourroudposht M, Idris A, Yusof, NM. A review of: Application of synthetic scaffold in tissue engineering heart valves. *Mater. Sci. Eng. C-Biomim*. 2015; 48:556–565.

7. Han F, Dong Y, Su Z, Yin R, Song A, Li S. Preparation, characteristics and assessment of a novel gelatin–chitosan sponge scaffold as skin tissue engineering material. *Int. J. Pharm*. 2014; 476:124–133.

8. Black CRM, Goriainov V, Gibbs D, Kanczler J, Tare RS, Oreffo ROC. Bone Tissue Engineering. *Curr. Mol. Bio. Rep*. 2015; 1:132–140.

9. Arahira T, Maruta M, Matsuya S, Todo M. Development and characterization of a novel porous β-TCP scaffold with a three-dimensional PLLA network structure for use in bone tissue engineering. *Mater. Lett*. 2015; 152:148–150.

10. Amini AR, Laurencin CT, Nukavarapu SP. Bone tissue engineering: Recent advances and challenges. *Crit. Rev. Biomed. Eng*. 2012; 40(5):363–408.

11. Bose S, Roy M, Bandyopadhyay A. Recent advances in bone tissue engineering scaffolds. *Trends Biotechnol*. 2012; 30:546–554.

12. Dash SR, Sarkar R, Bhattacharyya S. Gel casting of hydroxyapatite with naphthalene as pore former. *Ceram Int*. 2015; 41(3):3775–3790.

13. Bohner M, van Lenthe GH, Grunenfelder S, Hirsiger W, Evison R, Muller R. Synthesis and characterization of porous betal-tricalcium phosphate blocks. *Biomater*. 2005; 26(31):6099–6105.

14. de Sousa E, Motisuke M, Bertran CA. Obtenção e caracterização de espumas de cimento de fosfato de cálcio: avaliação dos métodos de emulsão e gelcasting. *Cerâm*. 2012; 58:500–503.

15. Tae-Kying R, Myeong-Jin O, Seung-Kwan M, Dong-Hyun P, Sung-Eun K, Jong-Hoon P, et. al. Uniform tricalcium phosphate beads with an open porous structure for tissue engineering. *Colloids Surf., B*. 2013; 112:368–373.

16. Baradararan S, Hamdi M, Metselaar, IH. Biphasic calcium phosphate (BCP) macroporous scaffold with different ratios of HA/β-TCP by combination of gel casting and polymer sponge methods. *Adv. Appl. Ceram*. 2012; 111(7):367–373.

17. Potoczek M, Zima A, Paszkiewicz Z, Slosarczyk A. Manufacturing of highly porous calcium phosphate bioceramics via gel-casting using agarose. *Ceram. Int*. 2009; 35(6):2249–2254.

18. Asif A, Nazir R, Riaz T, Ashraf N, Zahid S, Shahid R, et al. Influence of processing parameters and solid concentration on microstructural properties of gel-casted porous hydroxyapatite. *J. Porous Mater.* 2014; 21(1):31–37.

19. Santos CFL, Silva, AP, Lopes L, Pires I, Correia IJ. Design and production of sintered beta-tricalcium phosphate 3D scaffolds for bone tissue regeneration. *Mater. Sci. Eng. C-Biomim*. 2012; 32(5):1293–1298.

20. Janney MA, Nunn SD, Walls CA, Omatete OO, Ogle RB, Kirby GH, Mcmillan AD. Gelcasting. *In:* Rahman MN. The handbook of ceramic engineering. New York: Marcel Dekker; 1998. p.1–15.

21. Janney MA, Omatete OO, Walls CA, Nunn SD, Ogle RJ, Westmoreland G. Development of low-toxicity gelcasting systems *J. Am. Ceram. Soc*. 1998; 81(3):581–591.

22. Young AC, Omatete OO; Janney MA; Menchhofer PA. Gelcasting of alumina. *J. Am. Ceram. Soc*. 1991; 74(3):612–618.

23. Yang J, Yu J, Huang Y. Recent developments in gelcasting of ceramics. *J. Eur. Ceram. Soc.*2011; 31(14):2569–2591.

24. Fu Q, Saiz E, Rahaman MN, Tomsia AP. Bioactive glass scaffolds for bone tissue engineering: state of the art and future perspectives. *Mat. Sci. Eng. C-Biomim.* 2011; 31(7):1245–1256.

25. Chen QZ, Thompson ID, Boccaccini AR. 45S5 Bioglass® – derived glass- ceramic scaffolds for bone tissue engineering. *Biomater*. 2006; 27:2414–2425.

26. Cunha C, Sprio S, Panseri S, Dapporto M, Marcacci M, Tampieri A. High biocompatibility and improved osteogenic potential of novel Ca–P/titania composite scaffolds designed for regeneration of load-bearing segmental bone defects. *J. Biomed. Mater. Res. A.* 2013; 101(6):1612–1619.

27. Dorozhkin SV. Bioceramics of calcium orthophosphates. *Biomater.* 2010; 31:1465–1485.

28. Ratner B, Hoffman A, Schoen F, Lemons J. Biomaterials Science: An Introduction to Materials in Medicine. Canadá: Elsevier; 2013.

29. Carter C, Norton M. Ceramic Materials: Science and Engineering. USA: Springer; 2007.

30. Rosseta P, Deschaseauxc F, Layrolleb P. Cell therapy for bone repair. *Orthop. Traumatol. Surg. Res*. 2014; 100:S107–S112.

31. Chen Y, Wang J, Zhu XD, Tang ZR, Yang X, Tan YF, et al. Enhanced effect of b-tricalcium phosphate phase on neovascularization of porous calcium phosphate ceramics: In vitro and in vivo evidence. *Acta Biomater*. 2015; 11:435–448.

32. Elliot JC. Structure and chemistry of the apatites and other calcium orthophosphates. 1st ed. Amsterdam: Elsevier Science B.V; 1994.

33. Ryu HS, Youn HJ, Hong KS, Chang BS, Lee CK, Chung SS. An improvement in sintering property of β-tricalcium phosphate by addition of calcium pyrophosphate. *Biomater*. 2002; 23: 909–914.

34. Xue W, Dahlquist K, Banerjee A, Bandyopadhyay A, Bose S. Synthesis and characterization of tricalcium phosphate with Zn and Mg based dopants. *J. Mater. Sci. Mater. Med.* 2008; 19:2669–2677.

35. Ayed FB, Bouaziz J. Sintering of tricalcium phosphate–fluorapatite composites by addition of alumina. *Ceram. Int.* 2008; 34:1885–1892.

36. Acchar W, Ramalho EG. Effect of MnO_2 addition on sintering behavior of tricalcium phosphate: Preliminary results. *Mater Sci Eng. C-Biomim. 2008;* 28:248–252.

37. Pang YX, Bao X, Weng L. Preparation of tricalcium phosphate/alumina composite nanoparticles and self-reinforcing composites by simultaneous precipitation. *J. Mater Sci.* 2004; 39(20):6311–6323.

38. Ghomi H, Fathi MH, Edris H. Fabrication and characterization of bioactive glass/hydroxyapatite nanocomposite foam by gelcasting method. *Ceram. Int.* 2011; 37:1819-1824.

39. Lopes JH, Magalhães JA, Gouveia RF, Bertran CA, Motisuke M, Camargo SEA, Trichês ES. Hierarchical structures of β-TCP/45S5 bioglass hybrid scaffolds prepared by gelcasting. *J Mech Behav Biomed Mater.* 2016; 62:10-23.

40. Oliveira AP, Motisuke M, Leal CV, Beppu MM. A Comparative Study between β-TCP Prepared by Solid State Reaction and by Aqueous Solution Precipitation: Application in Cements. *KEM.* 2008; 361–363:355–358.

41. Karageorgiou V, Kaplan D. Porosity of 3D biomaterial scaffolds and osteogenesis. *Biomater*. 2005; 26:5474–5491.

42. Mosmann T. Rapid colorimetric assay for cellular growth and survival: application to proliferation and cytotoxicity assays. *J. Immunol. Methods.* 1983; 65:55–63.

43. Miller B, Pötter-Locher F, Seelbach A, Stopper H, Utesch D, Madle S. Evaluation of the in vitro micronucleus test as an alternative to the in vitro chromosomal aberration assay: position of the GUM Working Group on the in vitro micronucleus test. Gesellschaft für Umwelt-Mutations-forschung. *Mutat. Res.* 1998; 410:81–116.

44. Ayed FB, Bouaziz J. Sintering of tricalcium phosphate–fluorapatite composites with zirconia. *Journal of the European Ceramic Society.* 2008; 28:1995–2002.

45. Rehman HR, Zhang M. Preparation of porous hydroxyapatite scaffolds by combination of the gel-casting and polymer sponge methods. *Biomater.* 2003; 24:3293–3302.

46. Wu ZY, Hill RG, Yue S, Nightingale D, Lee PD, Jones JR. Melt-derived bioactive glass scaffolds produced by a gel-cast foaming technique. *Acta Biomater*. 2011; 7:1807–1816.

47. Bouslama N, Ayed FBen, Bouaziz J. Mechanical properties of tricalcium phosphate-fluorapatite-alumina composites. *Phys Procedia*. 2009; 2:1441-1448.

48. Ghzanfari SMH, Zamanian A. Phase transformation, microstructural and mechanical properties of hydroxyapatite/alumina nanocomposite scaffolds produced by freeze casting. *Ceram. Int.* 2013; 39:9835–9844.

49. Hesaraki S. Feasibility of alumina and alumina-silica nanoparticles to fabricate strengthened betatricalcium phosphate scaffold with improved biological responses. *Ceram. Int.* 2016; 42:7593–7604.

50. Gibson LJ, Ashby MF. Cellular solids: structure and properties. 2nd edn. Oxford: Pergamon; 1999. p. 429–452.

51. Neamat A, Gawish A, Gamal-Eldeen AM. Beta-Tricalcium phosphate promotes cell proliferation, osteogenesis and bone regeneration in intrabony defects in dogs. *Arch. Oral Biol.* 2009; 54:1083–1090.

52. Kim YH, Anirban JM, Song HY, Seo HS, Lee BT. In vitro and in vivo evaluations of 3D porous TCP-coated and non-coated alumina scaffolds. *J. Biomater App*. 2011; 25:539–558.

53. Lew KS, Othman R, Ishikawa K, Yeoh FY. Macroporous bioceramics: a remarkable material for bone regeneration. *J. Biomater App*. 2012; 27:345–358.

54. Tsaousi A, Jones E, Case CP. The *in vitro* genotoxicity of orthopaedic ceramic (Al_2O_3) and metal (CoCr alloy) particles. *Mutat. Res.* 2010; 697:1–9.